Are TrueFISP Images T_2/T_1-Weighted?

Teng-Yi Huang,[1,2] Ing-Jye Huang,[1,2] Cheng-Yu Chen,[2] Klaus Scheffler,[3] Hsiao-Wen Chung,[1,2*] and Hui-Cheng Cheng[4]

Images acquired using the TrueFISP technique (true fast imaging with steady-state precession) are generally believed to exhibit T_2/T_1-weighting. In this study, it is demonstrated that with the widely used half-flip-angle preparation scheme, approaching the steady state requires a time length comparable to the scan time such that the transient-state response may dominate the TrueFISP image contrast. Two-dimensional images of the human brain were obtained using various phase-encoding matrices to investigate the transient-state signal behavior. Contrast between gray and white matter was found to change significantly from proton-density- to T_2/T_1-weighted as the phase-encoding matrix size increased, which was in good agreement with theoretical predictions. It is concluded that TrueFISP images in general exhibit T_2/T_1-contrast, but should be more appropriately regarded as exhibiting a transient-state combination of proton-density and T_2/T_1 contrast under particular imaging conditions. Interpretation of tissue characteristics from TrueFISP images in clinical practice thus needs to be exercised with caution. Magn Reson Med 48:684–688, 2002. © 2002 Wiley-Liss, Inc.

Key words: TrueFISP; steady-state free precession; transient state; gray/white matter contrast

Rapid gradient-echo imaging with balanced gradient waveforms in all three gradient channels (SSFP or balanced FFE; referred to as TrueFISP for true fast imaging with steady-state precession in this article) (1–3) has recently generated significant attention in clinical practice. Combining the advantages of subsecond scan time per slice, high fluid-tissue contrast, 3D imaging compatibility, and inherent flow compensation, the TrueFISP technique has found applications in, for example, cardiac imaging (4), interventional radiology (5), whole-body screening (6), and fetal brain maturation (7). With advances in imaging options, such as magnetization preparation (8,9) or fat suppression (10), which provide versatile flexibility in image contrast, it is likely that the clinical use of TrueFISP will be further broadened in the future.

Image contrast in generic TrueFISP images is generally believed to be T_2/T_1-weighted (3,4,7,11,12). Indeed, as shown in early publications, the MR signal in the steady-state free precession (SSFP) regime with an SSFP angle of 180° can be expressed as (3,11,13):

$$\text{Signal} = M_0 \frac{(1 - e^{-TR/T1})\sin\alpha}{1 - e^{-TR/T1}\cos\alpha - e^{-TR/T2}(e^{-TR/T1} - \cos\alpha)}$$

[1]

where M_0 is the magnetization at thermal equilibrium and α is the flip angle. With TR $\ll T_1$ and TR $\ll T_2$, Eq. [l] reduces to:

$$\text{Signal} = M_0 \frac{\sin\alpha}{1 + \cos\alpha + (1 - \cos\alpha)(T1/T2)} \quad [2]$$

showing only T_2/T_1 dependency at large flip angles (e.g., α about 70°). When imaging the brain, for example, TrueFISP shows poor contrast between gray and white matter because the slight difference in their T_2/T_1 ratios partially cancels out differences in proton densities (3,7). It is partially because of this reason that application of the TrueFISP technique for brain imaging has not gained popularity as in body examinations. It is important to note, however, that Eqs. [1] and [2] hold true only when the data acquisition is carried out in the steady state. An early theoretical study on the duration of the transient phase of SSFP experiments demonstrated that the decay rate to the steady state is given by $-TR(T_2+2T_1)/T_1T_2$, and that the steady state is reached after about $5T_1T_2/(TR(T_2+2T_1))$ repetitions (14). The contrast of TrueFISP images may therefore depend on the transient-state behavior if approaching the steady state requires a time length comparable to the scan time.

In the present study, we show that even with the $(-\alpha/2)$–$(TR/2)$ preparation scheme commonly used in TrueFISP for rapid and smooth stabilization of the magnetization vector (15), the number of "preparatory" RF pulses needed to approach the steady state can exceed 100. As a result, the usual appearance of TrueFISP images should be more appropriately regarded as a transient-state combination of proton-density and T_2/T_1 contrast, a phenomenon similar to that found in other gradient-echo sequences (16,17). The actual image appearance depends on the number of RF pulses experienced by the magnetization prior to data acquisition near the center portion of the k-space.

MATERIALS AND METHODS

Two-dimensional transaxial images of the brain were acquired from seven healthy volunteers on a 1.5 T system (Siemens Vision+, Erlangen, Germany) using the True-FISP technique (TR/TE = 6.4/3.0 msec, one signal average) with 180° phase alternation of the excitation RF pulses

---

[1]Department of Electrical Engineering, National Taiwan University, Taipei, Taiwan, R.O.C.

[2]Department of Radiology, Tri-Service General Hospital and National Defense Medical Center, Taipei, Taiwan, R.O.C.

[3]Radiologische Universitaetsklinik Freiburg, Sektion "Bildgebende und Funktionelle Medizinische Physik," Freiburg, Germany.

[4]Veterans General Hospital-HealthTech Imaging Center, Taipei, Taiwan, R.O.C.

*Correspondence to: Hsiao-Wen Chung, Ph.D., Rm. 238, Department of Electrical Engineering, National Taiwan University, No.1, Sec. 4, Roosevelt Road, Taipei, Taiwan 10764, Taiwan, R.O.C. E-mail: chung@cc.ee.ntu.edu.tw

FIG. 1. Brain images acquired at a 70° flip angle with (**a**) 48, (**b**) 64, (**c**) 96, (**d**) 128, (**e**) 256, and (**f**) 768 RF pulses preceding data acquisition around the center of the *k*-space, respectively. Notice the decreasing contrast between gray and white matter from proton-density- to T_2/T_1-weighting as the number of preparatory RF pulses increases.
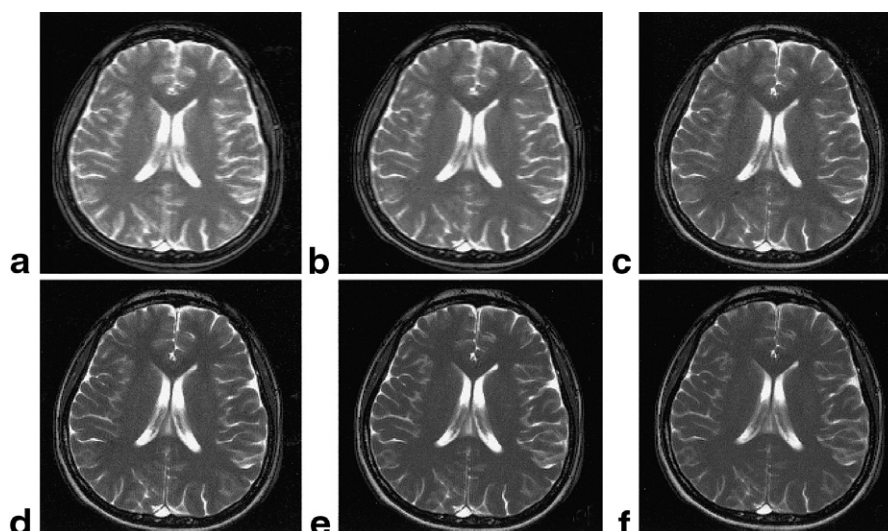
(i.e., SSFP angle = 180° for on-resonance spins). An initial RF pulse with $-\alpha/2$ flip angle was placed at TR/2 before the imaging pulse train to facilitate smooth evolution to the steady state (15). The order of phase encoding was linear, hence the image contrast, as dominated by the central portion of the *k*-space, was determined primarily by the magnetization having experienced about $N_p/2$ "preparatory" RF pulses, where N_p stands for the number of phase encoding. To examine the transient-state signal behavior, N_p was varied from 64 to 512 to mimic variations in the number of preparatory RF pulses (number of preparatory RF pulses = 32–256). Care was taken so that the spatial resolution was kept constant whenever possible, but we later found that the signal behavior was relatively independent of the spatial resolution. For some of the images, additional preparatory RF pulses were added by continuously scanning for more than one image at the same slice location. The flip angles for the excitation RF pulse were varied from 30° to 90° at 10° increments to investigate flip-angle dependency.

The theoretical behavior of MR signal intensity undergoing a continuous train of RF pulses, with $(-\alpha/2)$–(TR/2) preparation, was calculated for the same scanning parameters as that described for the imaging experiments. An ideal rectangular slice profile was assumed in the simulations. The possible effects of nonideal slice profiles will be discussed in a later section. Proton density, T_1, and T_2 values for the cerebrospinal fluid (CSF), gray matter, and white matter were measured from brain images of the subjects recruited for this study. Averaged values of the seven subjects were used for the calculation. T_1 values were estimated using an inversion recovery sequence at TR = 10 sec and by varying the inversion times. T_2 values were measured using a spin-echo sequence with 16 echoes at 22.5 msec separation. These tissue parameters were then estimated using nonlinear least-square fitting. The contrast between gray and white matter as derived above was compared with measurements from brain images.

RESULTS

Figure 1a–f shows brain images acquired at a 70° flip angle with 48, 64, 96, 128, 256, and 768 RF pulses preceding

data acquisition around the center of the *k*-space, respectively. Note the decrease in contrast between gray and white matter from proton-density- to T_2/T_1-weighting. Figure 2 shows the theoretical calculation of signal intensity for gray and white matter at a 70° flip angle, plotted as a function of the RF pulses preceding data acquisition around the center of the *k*-space. Approaching the steady state for gray ($T_1 \sim 1200$ msec; $T_2 \sim 100$ msec) and white matter ($T_1 \sim 900$ msec; $T_2 \sim 80$ msec) was faster than for CSF ($T_1 \sim 4500$ msec; $T_2 \sim 2200$ msec; data not shown), but still required about 150 preparatory RF pulses. For images at 256 phase encoding or lower, the image contrast is therefore a transient-state combination of proton-density and T_2/T_1, if using a linear phase-encoding order. This transient-state proton-density weighting accounts for the clearer contrast between gray and white matter in Fig.
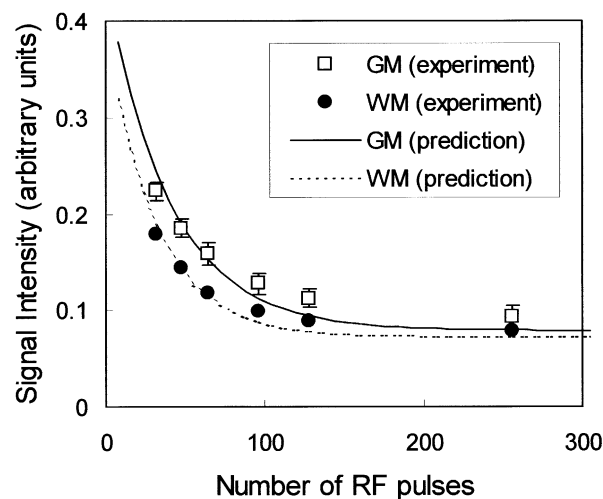

FIG. 2. Theoretical calculation of signal intensity for gray and white matter at a 70° flip angle, shown as a decreasing function of the number of RF pulses preceding data acquisition around the center of the *k*-space. Approaching the steady state requires about 150 preparatory RF pulses. Experimental data taken from the images in Fig. 1 demonstrate good agreement with the theoretical predictions.
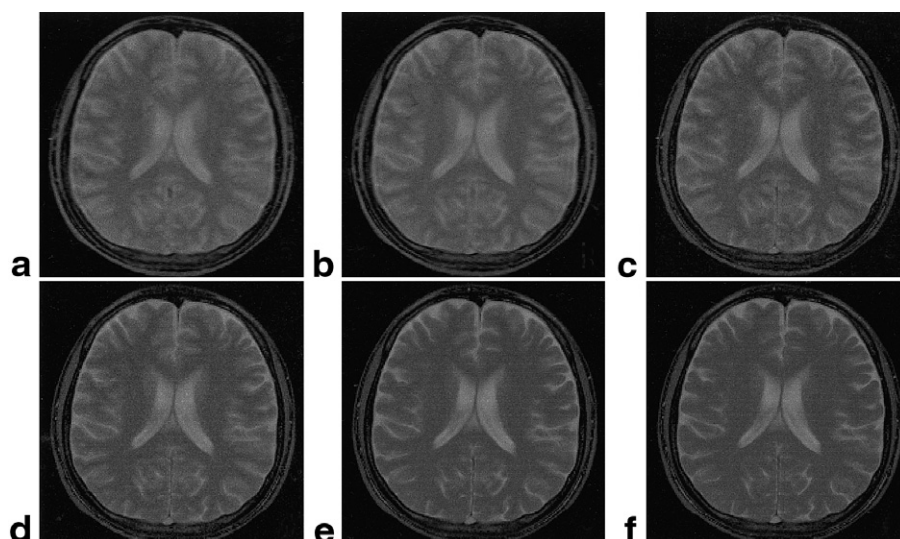
FIG. 3. Brain images acquired at a 30° flip angle with (**a**) 48, (**b**) 64, (**c**) 96, (**d**) 128, (**e**) 256, and (**f**) 768 RF pulses preceding data acquisition around the center of the *k*-space, respectively. Images are displayed with window settings identical to those used in Fig. 1. Compared with Fig. 1, these images do not exhibit visually significant variations in image contrast.

1a–c, which were acquired at low phase-encoding values. These results depart from the expectation of poor contrast from steady-state T_2/T_1-weighting. The experimental data (open squares and filled circles for gray and white matter in Fig. 2, respectively) taken from the images in Fig. 1 demonstrate good agreement with theoretical predictions.

Analogous to Fig. 1, Fig. 3a–f shows TrueFISP images of the brain acquired at a 30° flip angle with 48, 64, 96, 128, 256, and 768 RF pulses preceding data acquisition around the center of the *k*-space, respectively. Note that these images are displayed with window settings identical to those used in Fig. 1. Compared with images acquired using a 70° flip angle, the images in Fig. 3 do not exhibit visually significant variations in image contrast as a function of the number of preparatory RF pulses. In fact, we found that the images in Fig. 3 could be regarded as being equivalent when the operator was freely allowed to adjust the window settings. Figure 4 plots the theoretical prediction of the signal intensity for gray and white matter at a 30° flip angle, which again showed good agreement with the experimental data. Note that approaching the steady state using a 30° flip angle is slower than when using a 70° flip angle, requiring more than 250 RF pulses. In addition, when using a 30° flip angle, as the number of preparatory RF pulses increases, the change in signal intensity is relatively smaller compared with 70° excitations.

Figure 5 shows the contrast behavior between gray and white matter at flip angles of 30°, 50°, 70°, and 90°, respectively, plotted as a function of the number of preparatory RF pulses. The plot indicates that as the flip angle increases, changes in contrast with the number of RF pulses are more evident, although approaching the steady state seems to be faster. With a small number of preparatory RF pulses where the transient-state response dominates, contrast between gray and white matter increases as flip angle increases (Fig. 5, long arrow; images shown in Fig. 6). The opposite trend is seen with larger numbers of preparatory RF pulses (Fig. 5, short arrow; images not shown).

DISCUSSION

The results from this study demonstrate that images acquired using the TrueFISP technique actually exhibit a transient-state contrast combining proton-density- and T_2/T_1-weighting, if the $(-\alpha/2)$–(TR/2) preparation scheme (15) is used with a linear phase encoding order. In this regard, TrueFISP images are not strictly T_2/T_1-weighted in general, although the transient-state and steady-state contrast between fluids and parenchymal tissues are basically similar. The actual image appearance strongly depends on the number of RF pulses that precede data acquisition around the center of the *k*-space. The speed in reaching steady state also depends on tissue T_1 and T_2.

For fluids with a long T_1 and T_2, such as CSF, approaching the steady state is relatively slow. The amount of change in signal intensity is thus small during continuous
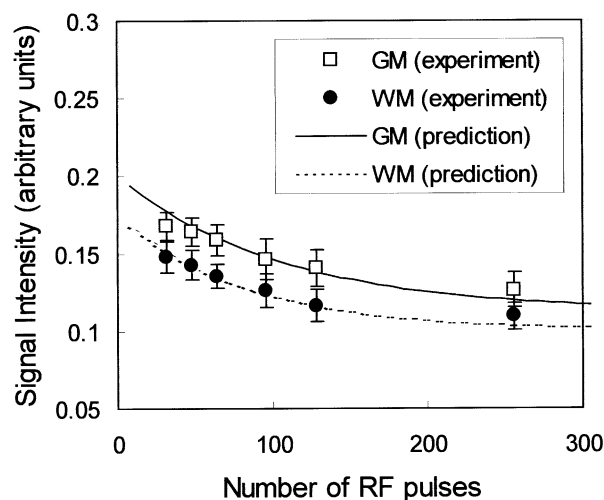

FIG. 4. Theoretical prediction of signal intensity for gray and white matter at a 30° flip angle, again showing good agreement with the experimental data. With a 30° flip angle the change in signal intensity is relatively smaller compared with 70° excitations (Fig. 2).
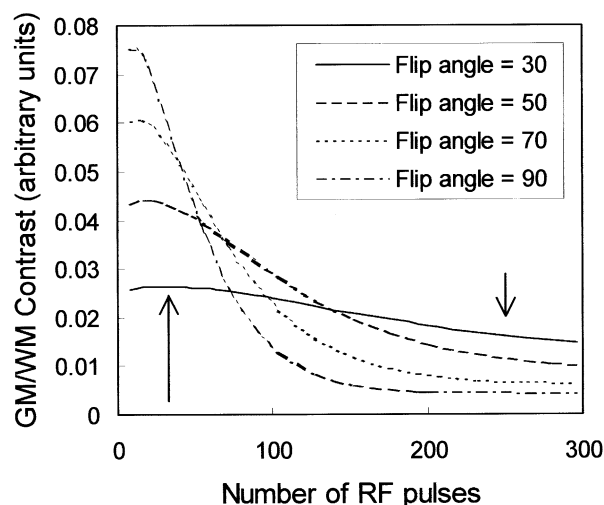
FIG. 5. Contrast behavior between gray and white matter at four flip angles as a function of the number of preparatory RF pulses. With a small number of preparatory RF pulses, gray/white matter contrast increases as flip angle increases (long arrow). The opposite trend is seen with larger numbers of preparatory RF pulses (short arrow).

data acquisition, making the transient-state behavior of fluids in TrueFISP images relatively unimportant. For parenchymal tissues, such as gray and white matter, the number of preparatory RF pulses needed to reach steady state is on the order of 100. Consequently, TrueFISP images acquired using different phase-encoding values (e.g., 128 vs. 512, standing for 64 and 256 preparatory RF pulses, respectively, if using a linear phase-encoding order) can show dramatic differences in contrast. This effect is particularly evident at large flip angles, as exemplified in Fig. 1. At smaller flip angles, on the other hand, since the term $(\cos\alpha)$ in Eq. [2] is close to unity, the contrast dependency on T_2/T_1 decreases and the image becomes primarily proton-density-weighted, even if acquired during the steady state. Therefore, the evolution of magnetization from transient-state proton-density weighting to steady-state proton-density weighting leads to visually insignificant differences in contrast as a function of the phase-encoding matrix (see Fig. 3).

The experimental data in this study were obtained solely from 2D TrueFISP images. For 3D TrueFISP imaging using a linear phase-encoding order, the number of RF pulses that precede data acquisition at the center of the 3D

k-space is on the order of thousands. The image contrast is anticipated to be determined by the steady-state behavior of the magnetization and is therefore T_2/T_1-weighted. In other words, for 3D TrueFISP imaging the transient-state behavior demonstrated in this study would not be observable if a linear view order were used. On the other hand, for segmented TrueFISP imaging, which is frequently employed in cardiac gating studies (4,18), the exact image contrast could contain a significant amount of transient-state contributions. Interpretation of tissue characteristics from TrueFISP images in clinical practice therefore needs to be exercised with caution and with these various considerations in mind. Furthermore, if centric phase encoding (17) is employed when using the TrueFISP technique, the resolution dependence of the transient-state contrast shown in this study may be tempered or even eliminated since the number of RF pulses experienced by the magnetization at the k-space center would be fixed at a constant.

There are some minor disagreements between our simulations and our experimental results (Figs. 2, 4). This discrepancy may be due to the fact that we assumed an ideal rectangular slice profile throughout our simulations, whereas in our actual imaging experiments the slice profile could, of course, not be ideally rectangular. A nonideal slice profile has the effect of lowering the true flip angle at the slice boundary, such that the transient-state behavior for real imaging experiments becomes a "weighted average," with the weighting scheme depending on the flip-angle distribution along the slice direction. Nevertheless, since the purpose of this study was to demonstrate the transient-state contrast in 2D TrueFISP images, we ignored the subtle effects of nonideal slice profiles because the phenomena of transient-state contrast exist regardless of the slice profiles used.

As a final note, the transient-state contrast investigated in this study applies only to TrueFISP imaging that employs the $(-\alpha/2)-(TR/2)$ preparation scheme widely used in commercialized clinical packages (15). There are other means to achieve rapid magnetization stabilization, such as the recently reported two-stage method for "catalyzing" (scaling and then directing) the magnetization vector (19). Whether the transient-state behavior significantly influences the image contrast in two-stage-catalyzed TrueFISP images remains an open question awaiting further investigation. Furthermore, throughout our theoretical calculations we assumed that a homogeneous static magnetic field can be obtained across the entire field-of-view via auto-
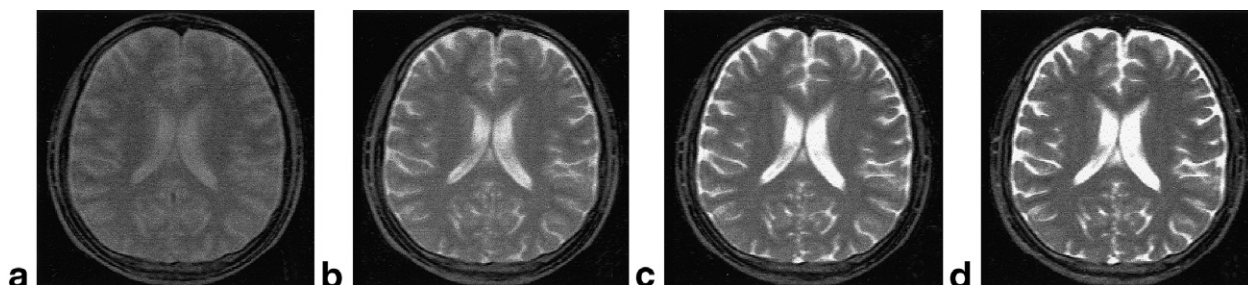

FIG. 6. Brain images acquired with 48 preparatory RF pulses at (**a**) 30°, (**b**) 50°, (**c**) 70°, and (**d**) 90° flip angles, respectively. Note that gray/white matter contrast increases as flip angle increases, as shown in Fig. 5.

matic shimming, such that transient-state artifacts due to off-resonance spins need not be considered. The assumption of field homogeneity is valid for our experimental conditions, as exemplified in Figs. 1 and 3, where no banding artifacts are seen in any of our TrueFISP images. Therefore, transient-state off-resonance artifacts previously reported for the $(-\alpha/2)$–$(TR/2)$ preparation scheme (19) are not present in our study since adequate shimming was readily achievable.

In conclusion, in the present study we found that with the $(-\alpha/2)$–$(TR/2)$ preparation scheme, the number of "preparatory" RF pulses needed for magnetization to approach the steady state is on the order of 100. Therefore, when using a linear phase-encoding order, particularly at large flip angles and depending on the phase-encoding value utilized, it may be more appropriate to consider 2D TrueFISP images as a transient-state combination of proton-density and T_2/T_1 contrast. Since the parenchymal contrast differs significantly between transient-state and steady-state imaging, interpretation of 2D TrueFISP images in clinical practice requires particular caution.

REFERENCES

1. Carr HY. Steady-state free precession in nuclear magnetic resonance. Phys Rev 1958;112:1693–1701.
2. Oppelt A, Graumann R, Barfuss H, Fischer H, Hartl W, Schajor W. FISP: a new fast MRI sequence. Electromedica 1986;54:15–18.
3. Haacke EM, Wielopolski PA, Tkach JA, Modic MT. Steady-state free precession imaging in the presence of motion: application for improved visualization of the cerebrospinal fluid. Radiology 1990;175:545–552.
4. Carr JC, Simonetti O, Bundy J, Li D, Pereles S, Finn JP. Cine MR angiography of the heart with segmented true fast imaging with steady-state precession. Radiology 2001;219:828–834.
5. Duerk JL, Lewin JS, Wendt M, Petersilge C. Remember true FISP? A high SNR, near 1-second imaging method for T_2-like contrast in interventional MRI at .2 T. J Magn Reson Imag 1998;8:203–208.
6. Barkhausen J, Quick HH, Lauenstein T, Goyen M, Ruehm SG, Laub G, Debatin JF, Ladd ME. Whole-body MR imaging in 30 seconds with real-time true FISP and a continuously rolling table platform: feasibility study. Radiology 2001;220:252–256.
7. Chung HW, Chen CY, Zimmerman RA, Lee KW, Lee CC, Chin SC. T2-weighted fast MR imaging with true FISP versus HASTE: comparative efficacy in the evaluation of normal fetal brain maturation. Am J Roentgenol 2000;175:1375–1380.
8. Scheffler K, Hennig J. T_1 quantification with inversion recovery TrueFISP. Magn Reson Med 2001;45:720–723.
9. Deshpande VS, Shea SM, Laub G, Simonetti OP, Finn JP, Li D. 3D magnetization-prepared true-FISP: a new technique for imaging coronary arteries. Magn Reson Med 2001;46:494–502.
10. Scheffler K, Heid O, Hennig J. Magnetization preparation during the steady state: fat-saturated 3D TrueFISP. Magn Reson Med 2001;45:1075–1080.
11. Zur Y, Stokar S, Bendel P. An analysis of fast imaging sequences with steady-state transverse magnetization refocusing. Magn Reson Med 1988;6:175–193.
12. Merrifield R, Keegan J, Firmin D, Yang GZ. Dual contrast TrueFISP imaging for left ventricular segmentation. Magn Reson Med 2001;46:939–945.
13. Freeman R, Hill HDW. Phase and intensity anomalies in Fourier transform NMR. J Magn Reson 1971;4:366–383.
14. Vassiliadis K, Sergiadis G. The duration of transient in SSFP experiments (abstr). In: Proc 12th Annual Meeting SMRM, New York, 1993. p 1208.
15. Deimling M, Heid O. Magnetization prepared true FISP imaging (abstr). In: Proc 2nd Annual Meeting SMR, San Francisco, 1994. p 495.
16. Holsinger AE, Riederer SJ. The importance of phase-encoding order in ultra-short TR snapshot MR imaging. Magn Reson Med 1990;16:481–488.
17. Holsinger-Bampton AE, Riederer SJ, Campeau NG, Ehman RL, Johnson CD. T1-weighted snapshot gradient-echo MR imaging of the abdomen. Radiology 1991;181:25–32.
18. Pereles FS, Kapoor V, Carr JC, Simonetti OP, Krupinski EA, Baskaran V, Finn JP. Usefulness of segmented trueFISP cardiac pulse sequence in evaluation of congenital and acquired adult cardiac abnormalities. AJR Am J Roentgenol 2001;177:1155–1160.
19. Hargreaves EA, Vasanawala SS, Pauly JM, Nishimura DG. Characterization and reduction of the transient response in steady-state MR imaging. Magn Reson Med 2001;46:149–158.